Advanced Physics Research

ADVANCED PHYSICS RESEARCH

www.advphysicsres.com

RESEARCH ARTICLE OPEN ACCESS

Anomalous Magnetization Dynamics After Dual Optical Excitation

Sergii Parchenko[1] | Peter M. Oppeneer[2] | Andreas Scherz[1]

[1]European XFEL, Schenefeld, Germany | [2]Department of Physics and Astronomy, Uppsala University, Uppsala, Sweden

Correspondence: Sergii Parchenko (sergii.parchenko@xfel.eu)

Received: 13 May 2025 | **Revised:** 21 November 2025 | **Accepted:** 27 November 2025

Keywords: dual optical excitation | inverse Faraday effect | ultrafast spin dynamics

ABSTRACT

Ultrafast optical excitation is widely used to manipulate electronic and magnetic properties of materials on femtosecond timescales. In this study, we investigate the response of copper to circularly polarized femtosecond pulses using time-resolved magneto-optical Kerr effect measurements. We compare the dynamics induced by single-pulse excitation with those resulting from a dual-pump configuration, in which two pulses arrive simultaneously from different directions. Although the individual contributions of the two pumps are similar when applied separately, their combined effect leads to a marked change in the spin/orbital dynamics. Specifically, we observe an approximately 2.5-fold increase in the decay time of the spin/orbital imbalance signal under dual-pump excitation. This result indicates that the joint action of two optical pulses can qualitatively alter the relaxation pathways in the system, beyond a simple additive response. The observed behavior highlights a previously unexplored regime of light-induced dynamics and suggests new strategies for controlling ultrafast processes in solids.

1 | Introduction

Ultrafast optical excitation has emerged as a powerful tool for controlling quantum states in materials, enabling precise manipulation of electronic, magnetic, and structural properties on femtosecond timescales [1, 2]. The ability to initiate and probe rapid transitions between quantum states has opened new frontiers in fields such as ultrafast magnetism [3–6], spintronics [7–9], and quantum systems [10–12]. By leveraging femtosecond laser pulses, researchers can transiently alter material properties, such as magnetization and charge transport, providing insights into the fundamental interactions governing quantum systems. In magnetically ordered materials, ultrafast optical excitation has been shown to induce a variety of dynamic responses, including ultrafast demagnetization [13, 14], magnetization precession [15], all-optical magnetization switching [16, 17] and other ultrafast magnetic processes [18–20]. Ultrafast optical excitation in metals drives the electronic system out of equilibrium, leading to non-thermal electron distributions and initiating complex relaxation dynamics involving energy transfer to phonons and spins [21, 22]. While the coupling between these subsystems can evolve in time, a key assumption often made is that the material's response is governed primarily by the absorbed energy, not by the detailed characteristics of the excitation geometry. In particular, if single-pulse excitations with different incidence angles or polarization states yield indistinguishable responses, it is reasonable to expect that a dual-pulse excitation composed of those same individual pulses would produce a response that simply scales with total fluence or absorbed energy.

However, recent studies using simultaneous dual-pump excitation, two femtosecond pulses arriving from different directions with identical polarization, report measurable deviations from single-pulse behavior in ferromagnetic metals. In magnetically ordered metallic materials, dual-pump excitation has been shown to significantly alter magnetization dynamics, including

increased recovery times after demagnetization [23], reduced threshold fluences for all-optical switching [24], and extended lifetimes of magnetization precession [25]. Such results indicate that the combined action of two pulses cannot be described solely by simple fluence scaling, pointing instead to an altered spin-lattice relaxation pathway under dual-pulse conditions. The observed change in relaxation dynamics may reflect a transient modification of electronic quantities depending on electron's orbital occupation numbers, such as spin–orbit coupling, that become influenced by the combined excitation geometry. The simultaneous arrival of two pulses from different directions could furthermore alter the local symmetry or coherence of the excited electrons, thereby influencing spin- and orbital-lattice scattering rates and angular momentum transfer efficiency.

In previous studies, the investigations were focused on magnetically ordered materials; hence, the probed magnetic signal represents the dynamics of long-range magnetic arrangement. However, if the local symmetry of the electron spin/orbital state is disturbed in a different way by dual optical excitation, the anomalous dynamics should be noticeable already on the level of interaction between individual electrons and the lattice, independently of long-range magnetic order. To explore this hypothesis, we carry out investigations on nonmagnetic copper, a material devoid of long-range magnetic order and collective spin interactions. In this study, we use circularly polarized ultrashort laser pulses to induce spin and orbital dynamics in copper via the inverse Faraday effect (IFE), a process that generates a transient magnetic moment in response to optical excitation [26, 27]. We compare the dynamics induced by single-pulse and dual-pump excitation, revealing a striking increase in the relaxation time of the induced magnetic moment under dual-pump conditions. Our data reveal an approximately 2.5× slower decay of the IFE-induced magnetic signal under dual-pump excitation, implying a modified angular momentum transfer rate compared to the single-pulse case. While the precise microscopic mechanism remains undetermined, this observation clearly shows that dual-pulse excitation leads to non-additive changes in spin- and orbital-lattice relaxation. The observation of altered relaxation dynamics in nonmagnetic copper under dual-pulse excitation raises the possibility that similar effects could occur in a broader range of materials. This invites further investigation into how excitation geometry influences ultrafast relaxation across different electronic systems.

2 | Results

2.1 | Experimental Configuration

Figure 1a shows the sketch of the experimental setup used in this study to measure the transient spin dynamics in Cu. Further details about the experimental configuration are given in the experimental section. Optical excitation was carried out with $\lambda = 1030$ nm circularly polarized pump pulses. Pump 1 was incident on the sample at an angle of 2° and the pump 2 beam had an angle of 60°. The circular polarization was obtained with a zero-order quarter-wave plate. During the dual pump experiments, both pumps had the same chirality of circular polarization. The change in magnetization state was monitored with a much weaker, time-delayed $\lambda = 515$ nm probe pulse, obtained by frequency doubling of the fundamental wavelength of the laser with a beta barium borate crystal. The incidence angle of the probe beam was 5° to the sample normal. The access to the time-resolved change in magnetization is realized via analysis of the rotation of the polarization of the probe pulse, making use of the magneto-optical Kerr effect in polar geometry and measured with a balanced photodiode. In this geometry, we measure the projection of the magnetic moment induced by pump pulses onto the wavevector of the probe light. Simultaneously, the time-resolved change in reflectivity was measured with a separate photodiode. All experiments were performed at room temperature and without an applied external magnetic field. The sample is a commercially available 5 × 5 × 1 mm one-sided polished single crystal of Cu with [110] being the out-of-plane direction.

2.2 | Inverse Faraday Effect Overview

The IFE refers to the interaction between circularly polarized light and electrons in a material, where the light induces a change in the electron's spin state [26, 27]. When circularly polarized light interacts with the electrons in a metal, it affects their orbital motion [28, 29, 31–33]. While it was long thought that the IFE primarily resulted in a light-induced spin polarization, recent ab initio calculations have shown that the dominant effect is in fact a light-induced orbital polarization [29]. The induced orbital polarization exists even without spin–orbit coupling, whereas spin–orbit coupling is required to create an optically induced spin polarization from the light induced orbital polarization. In Cu, the calculated orbital IFE is at least an order of magnitude larger than the spin IFE [29]. The circularly polarized light leads to an alteration in the orbital motion and induces a large orbital moment, which, mediated by spin–orbit coupling, causes the spins of the electrons to flip. The result is an imbalance between the orbital occupation numbers and spin-up and spin-down occupations of the electrons, which leads to a transient change in the magnetic state of the material [30]. However, it is important to note that this imbalance in the spin and orbital populations does not result in the formation of macroscopic magnetic order. Instead, the induced imbalance is a transient phenomenon, occurring on a sub-picosecond timescale, which does not lead to long-range magnetic moment alignment. As a result, the IFE provides a mechanism by which light can influence the electrons' spin and orbital polarizations on ultrafast timescales without the need for external magnetic fields [34, 35]. The IFE has become a key phenomenon in the field of ultrafast magnetism, offering a tool for selective excitation of magnetization dynamics. Indeed, IFE has been used in experiments to study magnetization precession [36], to perform deterministic control of magnetization states [37], and is considered to be important for multi-pulse magnetization switching [38], making it highly relevant for applications in optomagnetic devices and spintronics [39].

2.3 | Single Pump Dynamics

In Figure 1b, the transient Kerr rotation signal, $\Delta\theta_{\mathrm{Kerr}}$, is displayed for a single circularly polarized pump pulse (Pump 1) with two distinct helicities, measured at a fluence of 16.9 mJ/cm^2. The

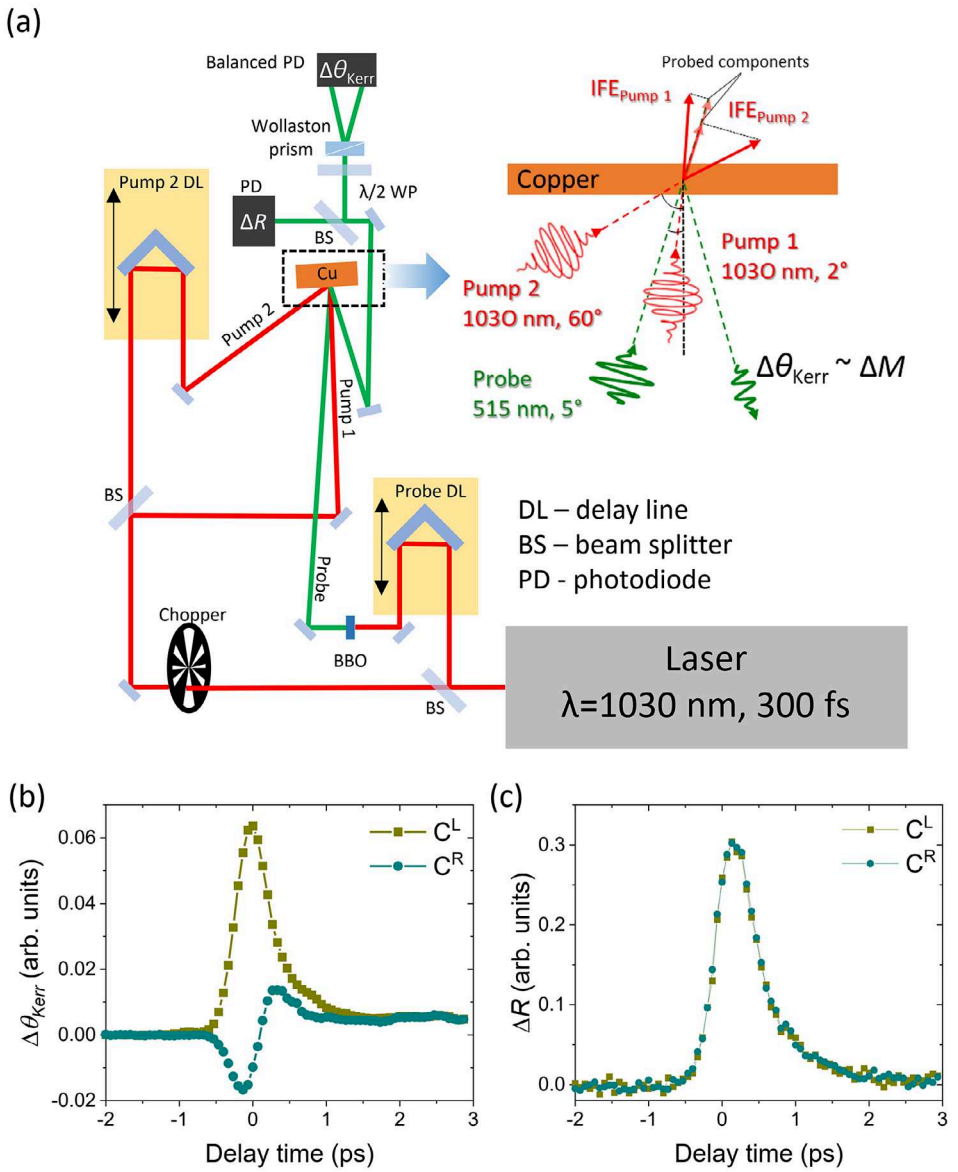

FIGURE 1 | (a) Experimental geometry for dual-pump time-resolved experiments. (b) and (c) Time-resolved differential polar Kerr signal and transient reflectivity of Cu, respectively, as a function of delay time after excitation with Pump 1 only with two different helicities of circular polarization and having a fluence of 16.9 mJ/cm^2.

Kerr rotation signal is sensitive to changes in the electronic spin and orbital populations, reflecting the material's magnetization dynamics. The IFE alters these spin and orbital populations, inducing a transient change in the material's magnetic state. The differing traces arise from IFE-induced magnetization, where circularly polarized light of opposite helicities generates magnetization with opposing orientations. Ideally, this should produce peak-like Kerr rotation signals with identical amplitudes and shapes but opposite signs. However, the observed signals exhibit asymmetry, consistent with prior studies using similar experimental conditions [40]. This asymmetry does not stem from variations in excitation efficiency between the two helicities, as confirmed by the transient reflectivity data (Figure 1c), which show no significant differences between the two helicities. Instead, we attribute the asymmetry to a nonmagnetic contribution, detailed further in the Experimental Section.

The magnetic contribution can be isolated by subtracting the time traces measured with the opposite helicity of circular polarization:

$$\Delta M(t) \propto \Delta\theta_{Kerr}^{C^L}(t) - \Delta\theta_{Kerr}^{C^R}(t) \quad (1)$$

where $\Delta\theta_{Kerr}^{C^{L(R)}}(t)$ represents the time-resolved Kerr rotation signal measured when the pump beam is left(right)- handed circularly polarized. The resulting signal, shown in Figure 2a, was derived using the data from Figure 1b and depicts the magnetization dynamics after single-pulse excitation with Pump 1 at a fluence of 16.9 mJ/cm^2. The resulting magnetization signal reflects the imbalance between the orbital populations and the number of spin-up and spin-down electrons, which are induced by the inverse Faraday effect (IFE). The data exhibits two key components: a peak-like signal at zero delay time, corresponding to the IFE-induced magnetization during the pulse excitation

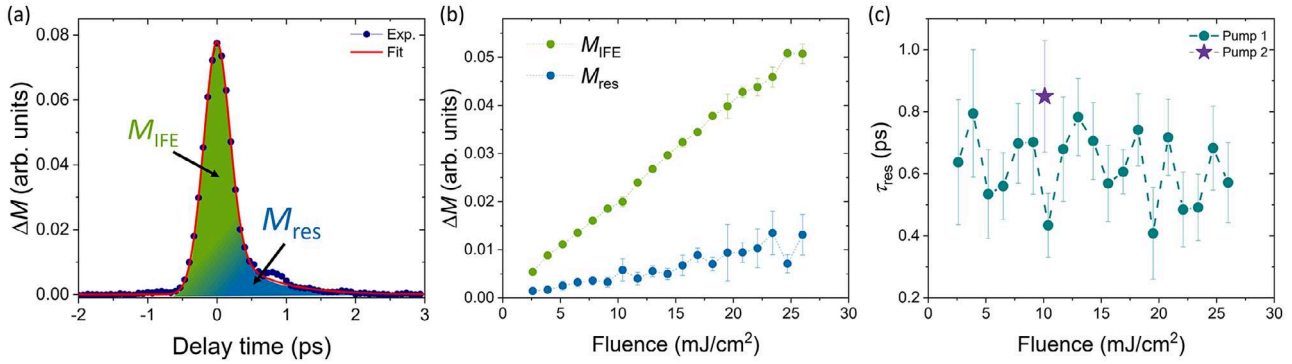

FIGURE 2 | (a) Light-induced magnetization as a function of time after excitation of Cu with Pump 1 only with a fluence of 16.9 mJ/cm^2. M_{IFE} and M_{res} components are indicated with green and blue, respectively. The solid red line is a fit to Equation (2). (b) Amplitudes of IFE M_{IFE} and residual magnetization M_{res}, and (c) decay time of residual magnetization τ_{res} as a function of fluence. The error bars are a 95 % confidence interval.

(shaded in green), and an additional exponential recovery of the residual magnetization imbalance (shaded in blue). The time-resolved magnetization traces were fitted with a combination of a Gaussian peak and exponential decay functions to capture both components:

$$\Delta M(t) = \Delta M_{IFE} e^{(t/\tau)^2} + \left\{ \left(\Delta M_{res} e^{-t/\tau_{res}} \right) g(t) \right\} \otimes \Gamma(t) \qquad (2)$$

where ΔM_{IFE} and $\Delta M_{(res)}$ are the amplitudes of the IFE and residual magnetization components, τ_{res} is the decay time of the residual magnetization, $g(t)$ is a step function, and $\Gamma(t)$ represents the convolution of the fit function with the Gaussian laser pulse. Figure 2b shows the amplitude of the IFE signal, ΔM_{IFE} (green), and the amplitude of the residual magnetic moment, ΔM_{res} (blue), as a function of pump fluence. Both amplitudes increase linearly with increasing fluence, with a constant ratio of ΔM_{IFE} / ΔM_{res} = 3.5. This linear increase is as expected since the IFE is an opto-magnetic effect, i.e., $\Delta M \propto E^2 \propto$Fluence, where E is the electric field strength. As pump fluence rises, the photon-induced spin and orbital polarizations increase, enhancing the magnetization imbalance and increasing both the ΔM_{IFE} and ΔM_{res} signals proportionally. Within the fluence regime during our experiments, we do not reach the nonlinear excitation regime [41]. The characteristic decay time of the residual magnetization imbalance, τ_{res}, quantifies the rate of angular momentum transfer from electrons to the lattice following optical excitation. Figure 2c shows τ_{res} as a function of pump fluence for single-pump excitation. Across all fluences, τ_{res} remains at approximately 0.6 ps, consistent with expectations for single-pump excitation [42]. This stability indicates that the angular momentum transfer efficiency is unaffected by light intensity. Notably, τ_{res} reflects the ability of individual electrons to transfer spin and orbital angular momentum to the lattice, independent of macroscopic magnetic order.

2.4 | Dual Pump Dynamics

In the dual optical excitation experiments, both Pump 1 and Pump 2 were circularly polarized with the same helicity, and the magnetic signal was extracted in the same manner as for single-pump excitation. The fluence for both pump beams was 10.1 mJ/cm^2. Figure 3 shows the transient magnetic signal ΔM as a function of delay time after excitation with Pump 1 only (yellow solid line) and Pump 2 only (blue solid line). The signal from the Pump 2 excitation closely resembles the dynamics induced by Pump 1, although the amplitude of ΔM for Pump 2 excitation is about half that of Pump 1. This reduction in amplitude is due to the experimental geometry, where the projection component of ΔM for Pump 2 is measured at an angle of 55° to the probe beam (see Figure 1a). The decay time for the Pump 2 excitation was found to be τ_{res} = 0.85 ± 0.18 ps (see Figure 2c), which is in good agreement with the decay time for Pump 1 excitation (see Figure 2c). This confirms that the individual effects of both pump beams on the electron dynamics are similar. However, when both pumps were applied simultaneously (dual-pump excitation), the transient magnetic response, shown in green, was noticeably different. The decay time increased to τ_{res} = 1.54 ± 0.22 ps, which is approximately 2.5 times larger than the decay time observed for single-pump excitation. Furthermore, when applying the same fitting procedure for dual-pump excitation, the obtained amplitude of the IFE-induced signal, ΔM_{IFE} (shown in green), was found to be about 3% smaller than the expected amplitude based

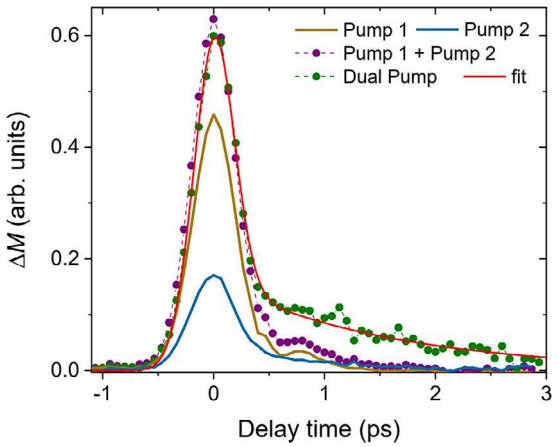

FIGURE 3 | Transient magnetic signal ΔM as a function of delay time after dual optical excitation (green), shown together with traces for individual Pump 1 (dark yellow) and Pump 2 (blue) excitation, as well as the linear superposition of signal from Pump 1 and Pump 2 (purple). The laser fluence of both pump pulses was 10.1 mJ/cm^2. The solid red line is a fit to Equation (2).

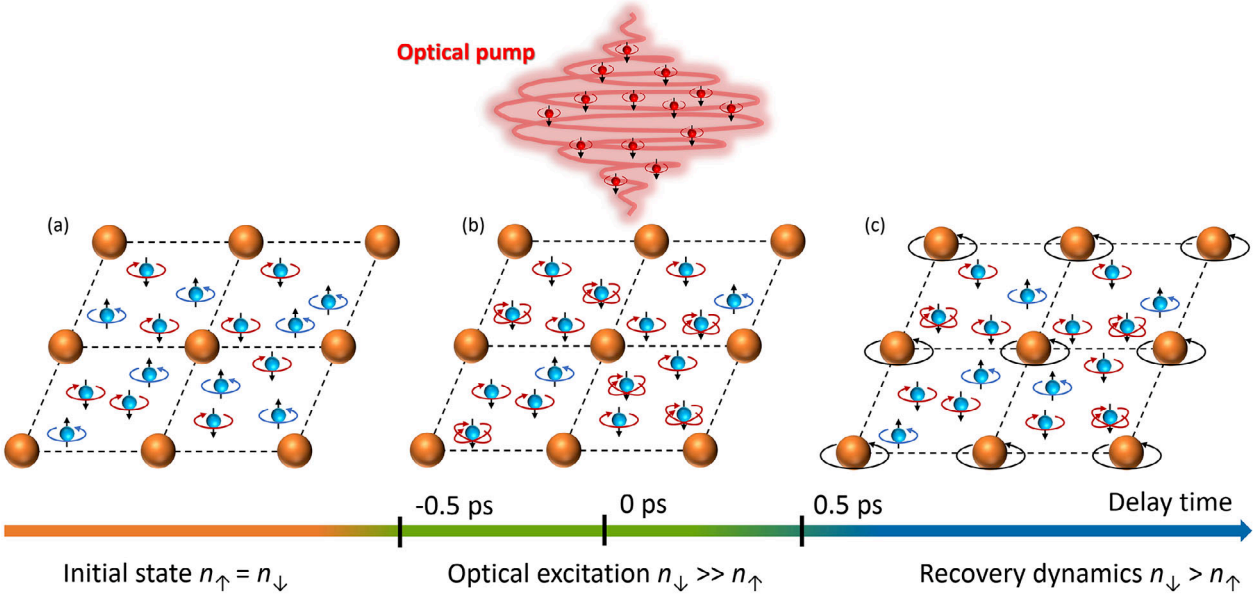

FIGURE 4 | Schematic representation of ultrafast spin/orbital dynamics in copper. Although the optical excitation is illustrated as a single circularly polarized pulse, the schematic represents dynamic steps that apply equally to both single- and dual-pump excitation. Panel (a) depicts the equilibrium state of copper, where a quenched orbital moment and equal numbers of spin-up and spin-down electrons result in no macroscopic magnetic moment. The spin of electrons (blue spheres) is indicated with black arrows and associated angular momentum with circular arrows in blue and red for opposite spin direction. The Cu ions are depicted with orange spheres. Panel (b) illustrates the state during optical excitation, where circularly polarized photons (red spheres) induce a modification of orbital state of electrons (shown by double circular arrows) and transient spin imbalance via the inverse Faraday effect—here, a small fraction of electrons is affected (the schematic exaggerates this for clarity). Panel (c) shows the recovery phase after the pump pulse, as the residual spin imbalance decays due to angular momentum transfer from the electrons to the lattice via the generation of polarized phonons.

on the linear superposition of the individual pump signals shown in purple, and the ratio $\Delta M_{\mathrm{IFE}} / \Delta M_{\mathrm{res}} = 3.1$ is somewhat smaller compared to single-pump experiments.

3 | Discussion

The observed difference between single- and dual-pump experiments is striking and challenges our fundamental understanding of spin- and orbital-polarized electron dynamics in metals after optical excitation. To gain a more intuitive understanding of these results, one can consider Figure 4, which schematically shows the different phases of the dynamical process. In equilibrium, copper exhibits no macroscopic magnetic moment, with a quenched orbital moment and an equal number of spin-up and spin-down electrons (Figure 4a). Upon optical excitation, a small fraction of electrons changes its orbital configuration (shown as double circular arrows in Figure 4) and undergoes spin flips, creating a transient magnetic moment, M_{IFE}, as shown in Figure 4b. For clarity, the number of spin flips in the schematic is exaggerated; in reality, optically induced magnetic moment is quite small. Calculations by Berritta et al. [29] show that the optically induced magnetic moment in Cu reaches approximately $2 \times 10^{-3}\,\mu_B$ per atomic volume under continuous-wave (CW) excitation at 1.55 eV with an intensity of 10 GW/cm^2. For pulsed excitation with a duration of ~300 fs and a fluence of 20.2 mJ/cm^2, corresponding to the combined fluence used in our dual-pump experiments, the peak magnetic moment can be estimated at approximately $1.5 \times 10^{-2}\,\mu_B$ considering both spin and orbital contributions. Most of this magnetization relax immediately after the laser pulse ends, with a small fraction retaining the angular momentum transferred from light during illumination. This residual magnetic moment M_{res} decays over time as electrons transfer angular momentum to the lattice by generating phonons with angular momentum, typically occurring on a sub-picosecond timescale [43, 44] (Figure 4c). The contradiction to our current understanding of electron dynamics in metals after optical excitation arises when considering the dynamics after the laser pulse ends. Whether the spin and orbital polarizations were created by a single pump or dual pumps, the electrons should, in principle, behave identically once the excitation is over. After approximately 0.5 ps, the electrons are no longer influenced by the pump light or any macroscopic magnetic arrangement and interact freely with their environment. Yet, the electrons excited by dual pumps exhibit significantly different dynamics, with a 2.5-fold increase in the decay time τ_{res}. The observed increase in relaxation time implies that dual-pulse excitation may transiently reduce the efficiency of angular momentum exchange between electrons and the lattice, potentially by influencing scattering pathways.

In dual-pump experiments where two coherent beams overlap, periodic excitation patterns can, in principle, arise from optical interference [45–50]. However, in our experimental configuration, several factors strongly mitigate the formation and impact of such interference patterns. Specifically, the two pump beams impinge on the sample at significantly different angles, one at normal incidence and the other at a grazing angle, resulting in an interference wave front that is tilted relative to the sample surface. This tilt, combined with the finite temporal and spatial overlap of the pulses, effectively smears out the interference

fringes on the sample surface. Numerical simulations performed for our geometry confirm that the modulation of the excitation intensity due to interference is mild, with the contrast between maxima and minima amounting to approximately 15% of the average non-interferometric intensity [23]. Moreover, even if a stronger periodic excitation pattern were present, its influence on the relaxation dynamics of the ΔM_{res} would likely be negligible. The spin system recovery is primarily controlled by spin-flip interactions with the lattice and occurs on nanometer length scales. Given the electron mean free path in copper (~40 nm), it is highly unlikely that a mild spatial modulation on the order of 1 μm would significantly affect spin relaxation dynamics or account for the observed factor-of-2.5 difference in relaxation times. Regarding the orbital decay channel, currently not much is known about the direct relaxation of orbital angular momentum to the lattice, how this process takes place and where phonons that can absorb angular momentum are located in the Brillouin zone.

3.1 | Mechanistic Insights

The anomalous increase in τ_{res} under dual-pump excitation reveals that angular momentum dissipation becomes significantly less efficient compared to the single-pulse case. Calculations of the electron-phonon thermalization in the related noble metal Au have shown that at a few ps time delay the phonon modes have not yet fully thermalized whereas the electronic system has [51]. While this implies that energy has been transferred from the electron system, an additional process is needed to dissipate spin and orbital angular momentum to the lattice. While for spin dissipation the relativistic Elliott–Yafet spin-flip scattering [52] will be active, orbital dissipation can be anticipated to involve different electron-phonon scattering channels. The reduced angular momentum dissipation in Cu suggests that dual-pulse excitation transiently reshapes the electron-phonon scattering phase space, potentially suppressing key pathways for both spin-lattice and orbital-lattice coupling. The persistence of this effect beyond the pump duration implies a longer lasting modification of the spin- and orbitally-polarized electronic state, driven not only by energy input but also by the spatial and temporal configuration of the excitation, highlighting a qualitatively different way to control electron-lattice interactions. The data presented here for Cu are consistent with previous experimental observations of spin dynamics in magnetically ordered materials, where dual optical excitation similarly reduced the efficiency of angular momentum transfer in various systems. For example, experiments on ultrafast demagnetization dynamics in Pt/Co/Pt and TbCo systems [23] revealed increased recovery times following ultrafast suppression of magnetization induced by dual-pump excitation compared to single-pulse excitation, occurring on picosecond timescales. Similarly, studies of magnetization precession in permalloy [25] showed prolonged decay times for magnetic oscillations triggered by dual-pump excitation compared to single-pump excitation, persisting for hundreds of picoseconds—far longer than any known light-induced modifications to electronic states in metals. These consistent trends observed across different materials and timescales suggest that the phenomenon may represent a general effect.

3.2 | Broader Implications

The demonstration of extended recovery dynamics of electrons' spin/orbital state in a nonmagnetic material is particularly intriguing. The lack of macroscopic magnetic order indicates that modification to the scattering channels is happening on the atomic scale and likely does not rely on the presence of long-range order, which indicates that various kinds of magnetic arrangements and couplings might be modified by dual optical excitation. The ability to modify the spin and orbital dynamics at the level of individual electrons through dual optical excitation opens exciting possibilities for controlling quantum states in materials. This technique could be harnessed to manipulate magnetization dynamics in ultrafast spintronic devices, where precise control over angular momentum transfer is essential. Moreover, the persistence of modified electron magnetization dynamics over nanosecond timescales suggests that dual optical excitation could enable long-lasting changes in a material's magnetic properties without altering the crystal structure. This presents an innovative, non-thermal route to functionalizing materials' properties for applications in optomagnetic devices and materials for quantum technologies. Although ultrafast excitation with a single pulse already alters electron scattering dynamics, our findings reveal that dual-pulse excitation modifies the spin-lattice and orbital-lattice relaxation dynamics in a fundamentally different manner. The significant change in angular momentum relaxation time implies that coherent dual-pulse excitation may access nontrivial electron configurations or electron-phonon scattering regimes that are not reachable with single-pulse excitation alone. This raises the possibility that the structure and symmetry of the excitation itself, not just the deposited energy, can transiently reshape how electrons interact with their environment, potentially pointing to a broader class of geometry-controlled ultrafast phenomena.

3.3 | Future Directions

While this study provides compelling evidence for the modification of electronic dynamics by dual optical excitation, there are still many questions to be addressed. For instance, is this effect specific to metals, or can it be observed in other nonmagnetic or magnetic materials? How do factors such as excitation wavelength and pulse duration influence the observed dynamics? Addressing these questions will require systematic experimental investigations across a range of materials and conditions, as well as theoretical work based on significantly more experimental data to develop models that explain the underlying mechanisms.

4 | Experimental Section

4.1 | Sample Preparation and Characterization

The sample used in this study was a commercial single crystal of copper (5 × 5 × 1 mm, [110] out-of-plane orientation) purchased from MTI Corporation. One side of the sample was polished to ensure a smooth, reflective surface suitable for laser excitation and measurements. No additional surface treatments were applied prior to the experiments.

4.2 | Laser System and Measurement Techniques

Ultrashort laser pulses were generated using an ActiveFiber laser system, delivering pulses with a central wavelength of 1030 nm, a duration of about 300 femtoseconds, and a repetition rate of 350 kHz. The fundamental wavelength for the pump (λ = 1030 nm) was chosen for its stability and avoids complications associated with frequency conversion. To produce a λ = 515 nm wavelength probe pulse for time-resolved measurements, we employed frequency doubling using a beta barium borate crystal. The dual-pump excitation setup utilized two laser pulses (Pump 1 and Pump 2) incident on the sample at angles of 2° and 60°, respectively. These angles were chosen to replicate the experimental geometry used in prior studies on magnetically ordered materials, ensuring consistency with earlier experiments. The beam radius was 250 μm for the pump and 100 μm for the probe at normal incidence. Circular polarization for pump pulses was obtained with a zero-order quarter-wave plate. The pump beam intensity was modulated with an optical chopper at 500 Hz maintaining the base repetition rate of the laser. This means that the sample was alternately exposed to a 2 ms window of continuous excitation at 350 kHz, followed by a 2 ms interval without optical excitation. Measurements were conducted at fluences 35% below the single-pump damage threshold of 35 mJ/cm^2 to ensure non-destructive conditions.

Magnetization dynamics was measured using a balanced photodiode setup to detect the transient polar Kerr rotation caused by the induced magnetization. The probe beam was split into vertically and horizontally polarized components using a Wollaston prism, and the difference in signal between the two components was measured to determine the polarization rotation of the probe beam. This rotation was directly sensitive to the magnetization of the sample. A narrow-band filter (520 nm ± 40 nm) was placed before the detector to ensure that only the 515 nm probe light was measured, eliminating any contamination from pump light or other wavelengths. However, when the sample is excited, there is also a change in reflectivity, which leads to a change in the overall intensity of the reflected probe beam. This change affects the difference signal on the balanced photodiode and causes an asymmetric shape of Kerr rotation signal for opposite helicity of the pump beam (see Figure 1b) but does not alter the interpretation of the data because we take the difference between traces taken with opposite helicity of the pump pulse to extract the magnetic signal. In addition to Kerr rotation measurements, transient reflectivity changes were monitored using a separate photodiode. Both signals were collected simultaneously using two lock-in amplifiers, enabling a precise correlation between magnetization dynamics and reflectivity changes under identical experimental conditions.

Acknowledgments

The authors express their sincere gratitude to Laura Heyderman for her valuable assistance in the final editing of the manuscript. This work was financially supported by the German Research Foundation (Deutsche Forschungsgemeinschaft) through CRC/TRR 227 "Ultrafast Spin Dynamics" (Project MF, Project ID No. 328545488), by the Swedish Research Council (VR), and by the Knut and Alice Wallenberg Foundation (Grants No. 2022.0079 and No. 2023.0336).

Open access funding enabled and organized by Projekt DEAL.

Conflicts of Interest

The authors declare no conflicts of interest.

Data Availability Statement

The data that support the findings of this study are available from the corresponding author upon reasonable request.

References

1. A. Kirilyuk, A. V. Kimel, and T. Rasing, "Ultrafast Optical Manipulation of Magnetic Order," *Reviews of Modern Physics* 82 (2010): 2731, https://doi.org/10.1103/RevModPhys.82.2731.

2. A. de la Torre, D. M. Kennes, M. Claassen, S. Gerber, J. W. McIver, and M. A. Sentef, "Colloquium: Nonthermal Pathways to Ultrafast Control in Quantum Materials," *Reviews of Modern Physics* 93 (2021): 041002, https://doi.org/10.1103/RevModPhys.93.041002.

3. B. Koopmans, G. Malinowski, F. Dalla Longa, et al., "Explaining the Paradoxical Diversity of Ultrafast Laser-Induced Demagnetization," *Nature Materials* 9 (2010): 259–265, https://doi.org/10.1038/nmat2593.

4. J.-Y. Bigot, M. Vomir, and E. Beaurepaire, "Coherent Ultrafast Magnetism Induced by Femtosecond Laser Pulses," *Nature Physics* 5 (2009): 515–520, https://doi.org/10.1038/nphys1285.

5. K. Légaré, G. Barrette, L. Giroux, et al., "Near-and mid-Infrared Excitation of Ultrafast Demagnetization in a Cobalt Multilayer System," *Physical Review B* 109 (2024): 094407.

6. Q. Remy, J. Hohlfeld, M. Vergès, et al., "Accelerating Ultrafast Magnetization Reversal by Non-Local Spin Transfer," *Nature Communications* 14 (2023): 445, https://doi.org/10.1038/s41467-023-36164-1.

7. T. Kampfrath, A. Kirilyuk, S. Mangin, S. Sharma, and M. Weinelt, "Ultrafast and Terahertz Spintronics: Guest Editorial," *Applied Physics Letters* 123 (2023): 050401, https://doi.org/10.1063/5.0167151.

8. A. El-Ghazaly, J. Gorchon, R. B. Wilson, A. Pattabi, and J. Bokor, "Progress Towards Ultrafast Spintronics Applications," *Journal of Magnetism and Magnetic Materials* 502 (2020): 166478, https://doi.org/10.1016/j.jmmm.2020.166478.

9. B. Dieny, I. L. Prejbeanu, K. Garello, et al., "Opportunities and Challenges for Spintronics in the Microelectronics Industry," *Nature Electronics* 3 (2020): 446–459, https://doi.org/10.1038/s41928-020-0461-5.

10. M. Buzzi, M. Först, R. Mankowsky, and A. Cavalleri, "Probing Dynamics in Quantum Materials with Femtosecond X-rays," *Nature Reviews Materials* 3 (2018): 299–311, https://doi.org/10.1038/s41578-018-0024-9.

11. A. Cavalleri, "Photo-Induced Superconductivity," *Contemporary Physics* 59 (2018): 31–46, https://doi.org/10.1080/00107514.2017.1406623.

12. D. Fausti, R. I. Tobey, N. Dean, et al., "Light-Induced Superconductivity in a Stripe-Ordered Cuprate," *Science* 331 (2011): 189–191, https://doi.org/10.1126/science.1197294.

13. E. Beaurepaire, J.-C. Merle, A. Daunois, and J.-Y. Bigot, "Ultrafast Spin Dynamics in Ferromagnetic Nickel," *Physical Review Letters* 76 (1996): 4250, https://doi.org/10.1103/PhysRevLett.76.4250.

14. A. Eschenlohr, M. Battiato, P. Maldonado, et al., "Ultrafast Spin Transport as Key to Femtosecond Demagnetization," *Nature Materials* 12 (2013): 332–336, https://doi.org/10.1038/nmat3546.

15. M. van Kampen, C. Jozsa, J. T. Kohlhepp, et al., "All-Optical Probe of Coherent Spin Waves," *Physical Review Letters* 88 (2002): 227201, https://doi.org/10.1103/PhysRevLett.88.227201.

16. C. D. Stanciu, F. Hansteen, A. V. Kimel, et al., "All-Optical Magnetic Recording with Circularly Polarized Light" *Physical Review Letters* 99 (2007): 047601.

17. S. Mangin, M. Gottwald, C.-H. Lambert, et al., "Engineered Materials for All-Optical Helicity-Dependent Magnetic Switching," *Nature Materials* 13 (2014): 286–292, https://doi.org/10.1038/nmat3864.

18. S. Baierl, M. Hohenleutner, T. Kampfrath, et al., "Nonlinear Spin Control by Terahertz-Driven Anisotropy Fields," *Nature Photonics* 10 (2016): 715–718, https://doi.org/10.1038/nphoton.2016.181.

19. T. Seifert, S. Jaiswal, U. Martens, et al., "Efficient Metallic Spintronic Emitters of Ultrabroadband Terahertz Radiation," *Nature Photonics* 10 (2016): 483–488, https://doi.org/10.1038/nphoton.2016.91.

20. C. S. Davies, F. G. N. Fennema, A. Tsukamoto, I. Razdolski, A. V. Kimel, and A. Kirilyuk, "Phononic Switching of Magnetization by the Ultrafast Barnett Effect," *Nature* 628 (2024): 540–544, https://doi.org/10.1038/s41586-024-07200-x.

21. P. Maldonado, K. Carva, M. Flammer, and P. M. Oppeneer, "Theory of Out-of-Equilibrium Ultrafast Relaxation Dynamics in Metals," *Physical Review B* 96 (2017): 174439, https://doi.org/10.1103/PhysRevB.96.174439.

22. M. Weißenhofer and P. M. Oppeneer, "Ultrafast Demagnetization Through Femtosecond Generation of Non-Thermal Magnons," *Advanced Physics Research* 4 (2024): 2300103.

23. S. Parchenko, M. Riepp, S. Marotzke, et al., "Demagnetization Dynamics After Noncollinear Dual Optical Excitation," *Physical Review B* 110 (2024): 054425, https://doi.org/10.1103/PhysRevB.110.054425.

24. S. Parchenko, A. Tsukamoto, P. M. Oppeneer, and A. Scherz, "Magnetization Switching in GdFeCo Induced by Dual Optical Excitation," *Physical Review B* 110 (2024): 174401, https://doi.org/10.1103/PhysRevB.110.174401.

25. S. Parchenko, D. Pecchio, R. Mondal, P. M. Oppeneer, and A. Scherz, "Magnetization Precession After Non-Collinear Dual Optical Excitation," *Journal of Applied Physics* 135 (2024): 173902, https://doi.org/10.1063/5.0191356.

26. J. P. van der Ziel, P. S. Pershan, and L. D. Malmstrom, "Optically-Induced Magnetization Resulting From the Inverse Faraday Effect," *Physical Review Letters* 15 (1965): 190, https://doi.org/10.1103/PhysRevLett.15.190.

27. P. S. Pershan, J. P. van der Ziel, and L. D. Malmstrom, "Theoretical Discussion of the Inverse Faraday Effect, Raman Scattering, and Related Phenomena," *Physical Review* 143 (1966): 574, https://doi.org/10.1103/PhysRev.143.574.

28. R. Hertel, "Theory of the Inverse Faraday Effect in Metals," *Journal of Magnetism and Magnetic Materials* 303 (2006): L1–L4, https://doi.org/10.1016/j.jmmm.2005.10.225.

29. M. Berritta, R. Mondal, K. Carva, and P. M. Oppeneer, "Ab Initio Theory of Coherent Laser-Induced Magnetization in Metals," *Physical Review Letters* 117 (2016): 137203, https://doi.org/10.1103/PhysRevLett.117.137203.

30. T. Adamantopoulos, D. Go, P. M. Oppeneer, and Y. Mokrousov, "Light-Induced Orbital and Spin Magnetism in 3 d, 4 d, and 5 d Transition Metals," *npj Spintronics* 3 (2025): 27.

31. D. Lian, Y. Yang, G. Manfredi, P.-A. Hervieux, and R. Sinha-Roy, "Orbital Magnetism Through Inverse Faraday Effect in Metal Clusters," *Nanophotonics* 13 (2024): 4291–4302, https://doi.org/10.1515/nanoph-2024-0352.

32. A. K. González-Alcalde, X. Shi, V. H. Ortiz, J. Feng, R. B. Wilson, and L. T. Vuong, "Enhanced Inverse Faraday Effect and Time-Dependent Thermo-Transmission in Gold Nanodisks," *Nanophotonics* 13 (2024): 1993–2002, https://doi.org/10.1515/nanoph-2023-0777.

33. M. Battiato, G. Barbalinardo, and P. M. Oppeneer, "Quantum Theory of the Inverse Faraday Effect," *Physical Review B* 89 (2014): 014413, https://doi.org/10.1103/PhysRevB.89.014413.

34. G.-M. Choi, A. Schleife, and D. G. Cahill, "Optical-Helicity-Driven Magnetization Dynamics in Metallic Ferromagnets," *Nature Communications* 8 (2017): 15085, https://doi.org/10.1038/ncomms15085.

35. S. Parchenko, K. Hofhuis, A. Å. Larsson, et al., "Plasmon-Enhanced Optical Control of Magnetism at the Nanoscale via the Inverse Faraday Effect," *Advanced Photonics Research* 6 (2025): 2400083, https://doi.org/10.1002/adpr.202400083.

36. A. V. Kimel, A. Kirilyuk, P. A. Usachev, R. V. Pisarev, A. M. Balbashov, and T. Rasing, "Ultrafast Non-Thermal Control of Magnetization by Instantaneous Photomagnetic Pulses," *Nature* 435 (2005): 655–657, https://doi.org/10.1038/nature03564.

37. B. Truc, A. A. Sapozhnik, P. Tengdin, et al., "Light-Induced Metastable Hidden Skyrmion Phase in the Mott Insulator Cu_2 $OSeO_3$," *Advanced Materials* 35 (2023): 2304197, https://doi.org/10.1002/adma.202304197.

38. M. S. El Hadri, M. Hehn, G. Malinowski, and S. Mangin, "Materials and Devices for All-Optical Helicity-Dependent Switching," *Journal of Physics D: Applied Physics* 50 (2017): 133002, https://doi.org/10.1088/1361-6463/aa5adf.

39. J. Walowski and M. Münzenberg, "Perspective: Ultrafast Magnetism and THz Spintronics," *Journal of Applied Physics* 120 (2016): 140901, https://doi.org/10.1063/1.4958846.

40. V. H. Ortiz, S. B. Mishra, L. Vuong, S. Coh, and R. B. Wilson, "Specular Inverse Faraday Effect in Transition Metals," *Physical Review Materials* 7 (2023): 125202, https://doi.org/10.1103/PhysRevMaterials.7.125202.

41. L. Lecherbourg, V. Recoules, P. Renaudin, and F. Dorchies, "Dynamics of Femtosecond Heated Warm Dense Copper with Time-Resolved L3-Edge XANES," *Philosophical Transactions of the Royal Society A: Mathematical, Physical and Engineering Sciences* 381 (2023): 20220214, https://doi.org/10.1098/rsta.2022.0214.

42. G.-M. Choi, H. G. Park, and B.-C. Min, "The Orbital Moment and Field-Like Torque Driven by the Inverse Faraday Effect in Metallic Ferromagnets," *Journal of Magnetism and Magnetic Materials* 474 (2019): 132–136, https://doi.org/10.1016/j.jmmm.2018.10.117.

43. C. Dornes, Y. Acremann, M. Savoini, et al., "The Ultrafast Einstein–de Haas effect," *Nature* 565 (2019): 209–212, https://doi.org/10.1038/s41586-018-0822-7.

44. S. R. Tauchert, M. Volkov, D. Ehberger, et al., "Polarized Phonons Carry Angular Momentum in Ultrafast Demagnetization," *Nature* 602 (2022): 73–77, https://doi.org/10.1038/s41586-021-04306-4.

45. P. Carrara, M. Brioschi, E. Longo, et al., "All-Optical Generation and Time-Resolved Polarimetry of Magnetoacoustic Resonances via Transient Grating Spectroscopy," *Physical Review Applied* 18 (2022): 044009, https://doi.org/10.1103/PhysRevApplied.18.044009.

46. J. Janušonis, T. Jansma, C. L. Chang, et al., "Transient Grating Spectroscopy in Magnetic Thin Films: Simultaneous Detection of Elastic and Magnetic Dynamics," *Scientific Reports* 6 (2016): 29143, https://doi.org/10.1038/srep29143.

47. G. Cao, S. Jiang, J. Åkerman, and J. Weissenrieder, "Femtosecond Laser Driven Precessing Magnetic Gratings," *Nanoscale* 13 (2021): 3746, https://doi.org/10.1039/D0NR07962F.

48. K. Yao, F. Steinbach, M. Borchert, et al., "All-Optical Switching on the Nanometer Scale Excited and Probed with Femtosecond Extreme Ultraviolet Pulses," *Nano Letters* 22 (2022): 4452–4458, https://doi.org/10.1021/acs.nanolett.2c01060.

49. D. Ksenzov, A. A. Maznev, V. Unikandanunni, et al., "Nanoscale Transient Magnetization Gratings Created and Probed by Femtosecond Extreme Ultraviolet Pulses," *Nano Letters* 21 (2021): 2905–2911, https://doi.org/10.1021/acs.nanolett.0c05083.

50. Y. Fan, G. Cao, S. Jiang, J. Åkerman, and J. Weissenrieder, "Spatiotemporal Observation of Surface Plasmon Polariton Mediated Ultrafast Demagnetization," *Nature Communications* 16 (2025): 873, https://doi.org/10.1038/s41467-025-56158-5.

51. U. Ritzmann, P. M. Oppeneer, and P. Maldonado, "Theory of Out-of-Equilibrium Electron and Phonon Dynamics in Metals After Femtosecond Laser Excitation," *Physical Review B* 102 (2020): 214305, https://doi.org/10.1103/PhysRevB.102.214305.

52. Y. Yafet, *Solid State Physics* (Academic, 1963): 59.